Effect of Screening of Intermicellar Interactions on the Linear and Nonlinear Rheology of a Viscoelastic Gel

Ranjini Bandyopadhyay* and A. K. Sood

Department of Physics, Indian Institute of Science, Bangalore 560 012, India

Received April 18, 2002. In Final Form: January 13, 2003

We report our studies of the linear and nonlinear rheology of aqueous solutions of the surfactant cetyl trimethylammonium tosylate (CTAT) with varying amounts of sodium chloride (NaCl). The CTAT concentration is fixed at 42 mM, and the salt concentration is varied between 0 and 120 mM. On increasing the salt (NaCl) concentration, we see three distinct regimes in the zero-shear viscosity and the high-frequency plateau modulus data. In regime I, the zero-shear viscosity shows a weak increase with salt concentration due to enhanced micellar growth. The decrease in the zero-shear viscosities with salt concentration in regimes II and III can be explained in terms of intermicellar branching. The most intriguing feature of our data, however, is the anomalous behavior of the high-frequency plateau modulus in regime II ($0.12 \leq [NaCl]/[CTAT] \leq 1.42$). In this regime, the plateau modulus *increases* with an increase in NaCl concentration. This is highly interesting, since the correlation length of concentration fluctuations and hence the plateau modulus G_0 are not expected to change appreciably in the semidilute regime. We propose to explain the changes in regime II in terms of a possible unbinding of the organic counterions (tosylate) from the CTA^+ surfaces on the addition of NaCl. In the nonlinear flow curves of the samples with high salt content, significant deviations from the predictions of the Giesekus model for entangled micelles are observed.

1. Introduction

The flow behavior of surfactant solutions has been studied extensively, both theoretically and experimentally.[1,2] Viscoelastic gels, which are formed by the entanglement of cylindrical micelles under appropriate conditions of temperature and salinity and in the presence of suitable counterions, can be used as model systems for rheological research. Even though the internal structures of these materials are often very complex, the viscoelastic parameters characterizing them are found to follow very simple scaling laws, making the prediction of their physical properties possible. In this paper, we focus on the effects of screening of intermicellar interactions, achieved by adding suitable amounts of the salt NaCl to cetyl trimethylammonium tosylate (CTAT) samples, on the linear and nonlinear rheology of the viscoelastic gel phase. The most interesting feature of this work is the existence of an anomalous regime of salt (NaCl) concentration where the high-frequency plateau modulus G_0 *increases* on the addition of salt. The maximum value of G_0 occurs when $[NaCl]/[CTAT] \sim 1.42$, where [NaCl] and [CTAT] represent the molarities of NaCl (60 mM) and CTAT (42 mM), respectively. Interestingly, even as the slope of G_0 changes sign on increasing salt concentration, there is no change in the slope of the relaxation time τ_R, while the slope of the zero-shear viscosity η_0 plotted versus salt concentration shows a significant decrease.

Theoretical and experimental studies on the effect of electrostatics on the growth of cylindrical micelles in the semidilute regime show a much stronger concentration dependence of the dynamical properties in salt-free conditions than in the highly screened case. Kern et al. have studied the effect of an increase in the concentration of the dimeric gemini surfactant on the micellar size, in the absence of added salt.[3] On increasing surfactant concentration c beyond the overlap concentration c^*, the zero-shear viscosity η_0 shows a very strong increase. In addition to this, the high-frequency plateau modulus G_0 shows a stronger concentration dependence than in the highly screened case ($G_0 \sim c^3$ for unscreened micelles, in contrast to the prediction $G_0 \sim c^{9/4}$ for highly screened, flexible micelles).[3] Experiments on cetyl trimethylammonium chloride (CTAC) in the presence of sodium salicylate (NaSal) show a tendency toward a monoexponential stress relaxation process with increase in the surfactant concentration c or a decrease in the temperature T.[4] In these experiments, the scaling relations for the zero-shear viscosity η_0 and the high-frequency plateau modulus G_0 are given by $\eta_0 \sim c^{1.1}$ and $G_0 \sim c^{1.7}$, where c is surfactant (CTAC) concentration. These scaling relations are found to be different from the theoretical model of Cates,[5] which predicts $\eta_0 \sim c^{3.7}$ and $G_0 \sim c^{2-2.3}$. These anomalies are explained in terms of the nonuniform distribution of the bound chloride and salicylate ions in the end-caps and along the lengths of the cylindrical micelles.[4] These experimental results prompted Mackintosh et al.[6] to analytically study the effect of electrostatics on the growth of cylindrical micelles. Considering the interaction of counterions with each other, the self-energy of the free charges, and the interaction of the counterions with the surface charge density to be the main contributions to the electrostatic repulsion between micelles, Mackintosh et al. find that charged, unscreened micelles exhibit three regimes of micellar growth with a tendency for very rapid

(1) Rehage, H.; Hoffmann, H. *Mol. Phys.* **1991**, *74*, 933.
(2) Cates, M. E.; Candau, S. J. *J. Phys.: Condens. Matter* **1990**, *2*, 5869.
(3) Kern, F.; Lequeux, F.; Zana, R.; Candau, S. J. *Langmuir* **1994**, *10*, 1714.
(4) Kern, F.; Zana, R.; Candau, S. J. *Langmuir* **1991**, *7*, 1344.
(5) Cates, M. E. *Macromolecules* **1987**, *20*, 2289. Cates, M. E. *J. Phys. Chem.* **1990**, *94*, 371.
(6) Mackintosh, F. C.; Safran, S. A.; Pincus, P. A. *Europhys. Lett.* **1990**, *12*, 697.

10.1021/la0203741 CCC: $25.00
Published on Web 03/15/2003

growth in the semidilute regime. Screened micelles, on the other hand, show a simple and more gradual power-law growth in the semidilute regimes.

2. Sample Preparation and Apparatus Used

Samples of CTAT/NaCl/water were prepared by weighing out the requisite quantity of CTAT in a microbalance and dissolving it in brine (solution of NaCl in deionized and distilled water) prepared at the following concentrations: 0, 0.5, 1, 2, 5, 10, 20, 40, 60, 80, 90, 100, and 120 mM. The concentration of CTAT in the brine solution was kept constant at 42 mM (1.9 wt %). The samples were kept in an incubator at 30 °C for a week and shaken frequently to ensure homogenization. All the experiments reported below were conducted at a fixed temperature of 25 °C. The oscillatory and flow measurements were performed in an AR 1000N stress-controlled rheometer (T. A. Instruments, U.K.), using a cone-and-plate geometry of radius 4 cm and angle 1° 59′. Sponges were used as solvent traps to prevent evaporation of the solvent (water) during the experiment.

3. Experimental Results

3.1. Linear Rheology. The dynamics of polymeric macromolecules is well understood in terms of the reptation model.[7,8] Experimentally, a purely exponential stress relaxation has been found in many surfactant solutions[1−4] where the dynamics obeys $\tau_{break} \ll \tau_{rep}$, where τ_{break} is the reversible breakage and reformation time of the micelle and τ_{rep} is its reptation (curvilinear diffusion) time. In such cases, the viscoelastic moduli of the material are given by the well-known Maxwell model[2,9] given by $G'(\omega) = G_0(\omega^2\tau_R^2)/(1 + \omega^2\tau_R^2)$ and $G''(\omega) = G_0(\omega\tau_R)/(1 + \omega^2\tau_R^2)$, where $G'(\omega)$ and $G''(\omega)$ are the elastic and viscous moduli, respectively, and the complex modulus $G^*(\omega) = G'(\omega) + iG''(\omega)$. In these equations, G_0 is the high-frequency plateau modulus, ω is the angular frequency of the applied oscillatory stress, and τ_R is a characteristic relaxation time of the sample given by $\tau_R = (\tau_{rep}\tau_{break})^{1/2}$. For a distribution of relaxation times, the stress relaxation may be fitted to a stretched exponential model given by

$$G(t) \sim \exp\left[-\text{constant} \times \left(\frac{t}{\tau_{rep}}\right)^{\alpha}\right] \qquad (1)$$

where the exponent α depends on the surfactant concentration, salinity, and temperature and tends to 1 when $\tau_{break} \ll \tau_{rep}$. In the frequency domain, the corresponding form is the empirical Cole−Davidson model,[10] where the complex relaxation $G^*(\omega)$ can be described as

$$G^*(\omega) = G_0\left[1 - \frac{1}{(1 + i\omega\tau_R)^{\alpha}}\right] \qquad (2)$$

where G_0 corresponds to $G(\omega \to \infty)$. G_0 can be used to estimate ξ, the correlation length of concentration fluctuations, by using the relation $G_0 \sim (k_BT/\xi^3)$.[2,11]

Figure 1 shows the frequency response ($G'(\omega)$ and $G''(\omega)$ vs ω) measurements for CTAT/NaCl/water for a few typical salt concentrations (c_{NaCl} = (a) 0 mM, (b) 20 mM, (c) 60 mM, and (d) 100 mM) over three decades of angular frequencies, and the corresponding fits to the real and imaginary parts of the Cole−Davidson form given by eq 2 (shown by solid lines in each plot).

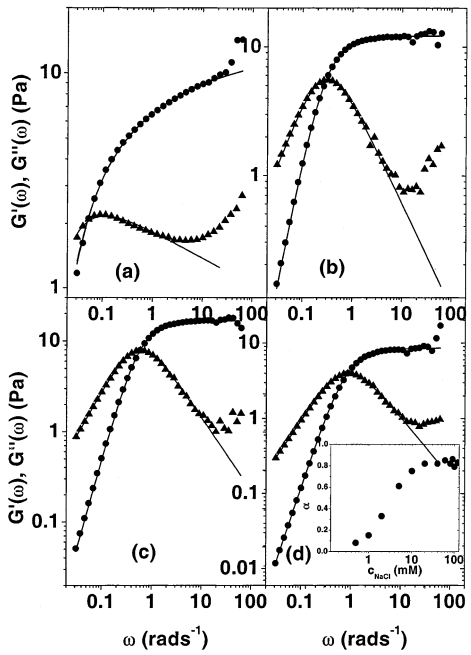

Figure 1. The frequency response curves ($G'(\omega)$ denoted by circles and $G''(\omega)$ denoted by triangles versus the angular frequency ω) of aqueous solutions of 42 mM CTAT + NaCl and their corresponding fits to the Cole−Davidson model (shown by solid lines). The CTAT concentration is maintained constant at 42 mM, while the NaCl concentrations corresponding to the graphs are (a) 0 mM, (b) 20 mM, (c) 60 mM, and (d) 100 mM. The inset of (d) shows the plot of the values of α obtained from the fits to the Cole−Davidson model vs the salt concentration c_{NaCl}.

The fits to the Cole−Davidson form of the frequency response data in the presence of 20−120 mM NaCl yield $\alpha \sim 0.80-0.90$, in comparison to the unscreened micellar phase (0 mM NaCl) where $\alpha \sim 0.15$. For the NaCl concentrations of 0.5, 1, 2, 5, and 10 mM, the values of α are found to increase with increasing molarity of the brine solution. The inset of Figure 1 shows the values of α obtained from the Cole−Davidson fit as a function of salt concentration, which indicates a gradual crossover from nonexponential to single-exponential stress relaxation on the addition of NaCl to CTAT solutions. Similar observations by Rehage et al.[1,12] on adding NaSal to cetylpyridinium chloride (CPyCl) solutions have been explained in terms of a crossover from diffusion-controlled to kinetically controlled stress relaxation processes. The fits shown in Figure 1 also give us estimates of the high-frequency plateau modulus G_0 and the terminal relaxation time τ_R. The values of τ_R have also been calculated from the crossover frequency ω_{co} using the relation $\tau_R = 1/\omega_{co}$ (Figure 4a). The data acquired in the presence of 20−120 mM NaCl can also be fitted satisfactorily to the Maxwell model[2] as is seen from the semicircular nature of the Cole−Cole plots ($G'(\omega)/G_0$ versus $G''(\omega)/G_0$ plotted in Figure 2). G_0 is the value of the high-frequency plateau modulus obtained from fits to the Cole−Davidson model.

The Cole−Cole plots for the CTAT samples with low salt content (≤5 mM) are found to deviate considerably from the semicircular behavior characteristic of a Maxwellian fluid. We note that these deviations at high frequencies ($\omega \geq \omega_b$) and the subsequent upturn ($\omega \geq \omega_e$) in the Cole−Cole plots are due to the reversible breaking

(7) deGennes, P. G. In *Scaling Concepts in Polymer Physics*; Cornell University Press: Ithaca, NY, 1979.
(8) Doi, M.; Edwards, S. F. In *The Theory of Polymer Dynamics*; Clarendon: Oxford, 1986.
(9) Fischer, P.; Rehage, H. *Rheol. Acta* **1997**, *36*, 13.
(10) Menon, N.; Nagel, S. R.; Venerus, D. C. *Phys. Rev. Lett.* **1994**, *73*, 963.
(11) Candau, S. J.; Hirsch, E.; Zana, R.; Delsanti, M. *Langmuir* **1990**, *5*, 1525.
(12) Rehage, H.; Hoffmann, H. *J. Phys. Chem.* **1988**, *92*, 4712.

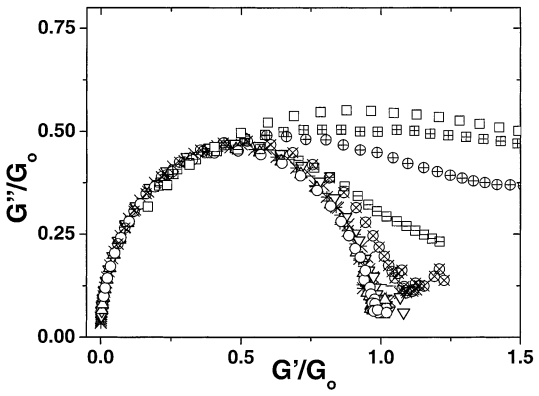

Figure 2. Normalized Cole−Cole plots obtained by plotting $G''(\omega)/G_0$ vs $G'(\omega)/G_0$ for CTAT (42 mM)/NaCl/water. The different symbols correspond to the following NaCl concentrations: (a) squares for 0 mM, (b) plus-centered squares for 0.5 mM, (c) plus-centered circles for 1 mM, (d) dash-centered squares for 2 mM, (e) ×-centered circles for 5 mM, (f) circles for 20 mM, (g) up-triangles for 40 mM, (h) down-triangles for 60 mM, (i) plus signs for 80 mM, (j) × signs for 90 mM, (k) * signs for 100 mM, and (l) − signs for 120 mM.

of the wormlike chains at a characteristic time τ_{break} and the contribution of the localized dynamics between entanglements (the Rouse modes), respectively.[13] The ratio $\varsigma = \tau_{break}/\tau_{rep}$, which compares the time scale for micellar breakage and reformation with that of reptative motion, can be estimated from the normalized Cole−Cole plot (Figure 2) by following the discussion of Granek et al. in ref 13. For the CTAT solutions with low salt content, the departure of the normalized Cole−Cole plot from the osculating circle and the observed linearity of the G''/G_0 versus G'/G_0 plot at high frequencies indicates a significantly large value of the ratio ς, which suggests a slow-breaking regime. Addition of salt results in an increasingly semicircular Cole−Cole plot, which indicates an increase in the breakage and reformation rate of the micelles. The comparatively large value of the ratio ς at low salt concentrations indicates the presence of a distribution of relaxation times and gives rise to a nonexponential stress relaxation process under these conditions. An exponential stress relaxation curve is obvious from the semicircular nature of the Cole−Cole plot at high salt concentrations, where stress relaxation is dominated by the micellar breakage dynamics.

The complex viscosity $\eta^*(\omega)$ may be written in terms of $G'(\omega)$ and $G''(\omega)$ as $\eta^*(\omega) = [(G'(\omega))^2 + (G''(\omega))^2]^{1/2}/\omega$. For viscoelastic gels, the complex viscosity is given by[9]

$$|\eta^*(\omega)| = \frac{\eta_0}{\sqrt{1 + \omega^2 \tau_R^2}} \tag{3}$$

where, for the Maxwell model, the zero-shear viscosity η_0 is given by $\eta_0 = G_0\tau_R$. Figure 3 shows the plots of the complex viscosities $\eta^*(\omega)$ (triangles) versus ω measured for the samples with c_{NaCl} equal to (a) 0 mM, (b) 20 mM, (c) 60 mM, and (d) 100 mM, versus the angular frequencies ω, and the corresponding fits to the model for giant wormlike micelles given in eq 3.[9] The fits, shown by dashed lines, are found to be poor for the unscreened case but agree very well with the experimental data for the samples with high concentrations of added salt ($c_{NaCl} \geq 20$ mM). The values of η_0 obtained from these fits are shown in Figure 4c by solid triangles. The model by Hess[14] describes the upturn of the Cole−Cole plot and may be used to predict G_0 and η_0 by fitting the entire frequency range.

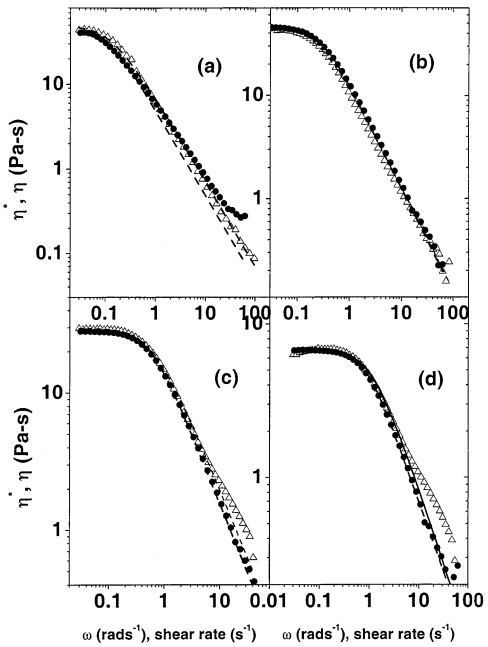

Figure 3. The normalized shear viscosity $\eta(\dot\gamma)/\eta_0$ (circles) and the normalized dynamic viscosity $\eta^*(\omega)/\eta_0$ (triangles) plots versus $\dot\gamma$ and ω for CTAT (42 mM)/NaCl/water samples. The NaCl concentration corresponding to each plot is as follows: (a) 0 mM, (b) 20 mM, (c) 60 mM, and (d) 100 mM. The solid lines show the fits to eq 3, and the dotted lines show the fits to the Giesekus model (eq 7).

3.2. Nonlinear Rheology. 3.2.1. The Giesekus Model. The Giesekus model[15] can be used to predict the nonlinear flow properties of surfactant solutions. This model uses the reptation theory as the starting point and introduces a deformation-dependent mobility tensor to account for the orientation effects of flow. This model gives us the following relations between rheological parameters such as the shear stress σ and the first and second normal stress differences N_1 and N_2 in the $t \rightarrow \infty$ limit:

$$\sigma(\infty, \dot\gamma) = \frac{G_0}{2\tau_R\dot\gamma}(\sqrt{1 + 4\tau_R^2\dot\gamma^2} - 1) \tag{4}$$

$$N_1(\infty, \dot\gamma) = 2G_0\frac{1 - \Lambda^2}{\Lambda} \tag{5}$$

$$N_2(\infty, \dot\gamma) = G_0(\Lambda - 1) \tag{6}$$

where

$$\Lambda^2 = \frac{\sqrt{1 + 4\tau_R^2\dot\gamma^2} - 1}{2\tau_R^2\dot\gamma^2}$$

In the Giesekus model, the shear viscosity $\eta(\dot\gamma)$ is given by

$$\eta(\dot\gamma) = \frac{\eta_0}{2\tau_R^2\dot\gamma^2}(\sqrt{1 + 4\tau_R^2\dot\gamma^2} - 1) \tag{7}$$

(13) Granek, R.; Cates, M. E. *J. Phys. Chem.* **1992**, *96*, 4758.

(14) Hess, S. *Physica A* (*Amsterdam*) **1979**, *87A*, 273.

(15) Giesekus, H. *J. Non-Newtonian Fluid Mech.* **1982**, *11*, 69.

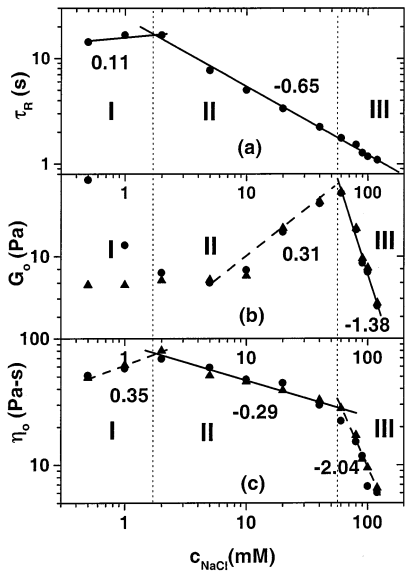

Figure 4. The values of τ_R, obtained from the crossover frequency ω_{co} of G' and G'', have been plotted in (a) vs c_{NaCl} (solid circles). In (b), we have plotted the values of G_0 obtained from the fits to the Cole−Davidson model (indicated by filled circles) and from the values of G' at $\omega = 29$ rads^{-1} (filled triangles). The deviation at low salt contents is because the plateau in G_0 has not been reached at the highest frequencies measured. Under these conditions, we are unable to calculate reliable values of G_0 as our rheometer is incapable of reaching high enough frequencies (the waveform of the response is found to get distorted at higher frequencies). (c) shows the plots of the zero-shear viscosities η_0 with increasing c_{NaCl}, obtained from the fits to the dynamic viscosity η^* (solid triangles) and the fits to the Giesekus model of the shear viscosity η (solid circles). The solid and dashed lines are the fits to $A \sim c_{NaCl}{}^{\beta}$, $A = \tau_R$, G_0 and η_0. The values of β in each regime are noted on the graphs.

3.2.2. Cox−Merz Rule. The Cox−Merz rule is a semiempirical rule which relates the complex viscosity $\eta^*(\omega)$ with the shear viscosity $\eta(\dot\gamma)$ as $\eta(\dot\gamma) = |\eta^*(\omega)|$, where $\omega = \dot\gamma$. The shear viscosity $\eta(\dot\gamma)$ is predicted by the Giesekus model and is given by eq 7. The dynamic viscosity may be calculated from the viscoelastic moduli using $\eta^*(\omega) = [(G'(\omega))^2 + (G''(\omega))^2]^{1/2}/\omega$ and may be fitted to eq 3. For the CTAB/NaSal (60 mM/350 mM) system forming giant wormlike micelles, a relatively good agreement to the Cox−Merz rule is observed.[9] Nonlinear rheology measurements have been used to estimate the zero-shear viscosity η_0 and the relaxation time τ_R from the flow curves. Here the shear stress σ and the viscosity η are measured simultaneously as a function of the shear rate $\dot\gamma$. Figure 3 shows the fits (shown by solid lines) to the Giesekus model (eq 7) of the shear viscosities $\eta(\dot\gamma)$ (indicated by filled circles) versus shear rates $\dot\gamma$ for the samples with salt content (a) 0 mM, (b) 20 mM, (c) 60 mM, and (d) 100 mM. For high salt concentrations, the fits to the Giesekus model are found to deviate considerably from the experimental data at high values of $\dot\gamma$. This may be explained by considering the fact that the Giesekus model considers only the orientational effects of the micelles and neglects the breaking and reformation of micelles that are dominant at high shear rates. The values of η_0 and τ_R obtained from these fits are compared to those obtained from the fits to $\eta^*(\omega)$ (Table 1). The values thus calculated from the linear and nonlinear rheology measurements deviate considerably from each other at low salt concentrations but show some agreement at $c_{NaCl} \geq 20$ mM.

Table 1. Parameters τ_R and η_0, Obtained from the Fits of $\eta^*(\omega)$ versus ω to Equation 3 (denoted by DV) and from the Fits of $\eta(\dot\gamma)$ versus $\dot\gamma$ to the Giesekus Model (Equation 7, denoted by GM)

NaCl (mM)	τ_R s (DV)	τ_R s (GM)	η_0 Pa s (DV)	η_0 Pa s (GM)
0	8.78	12.88	42.42	36.69
0.5	13.93	21.03	49.62	36.72
1	15.16	24.5	62.13	51.02
2	15.77	22.35	80.27	70.43
5	36.69	31.61	42.42	39.05
10	6.00	7.2	45.52	46.08
20	3.53	3.44	38.7	44.35
40	2.30	1.77	32.49	22.21
60	1.79	1.46	27.98	29.63
80	1.51	1.06	17.09	15.24
90	1.30	0.98	11.14	11.72
100	1.21	0.58	9.50	6.74
120	1.08	0.50	6.56	6.03

4. Discussion

In this section, we will attempt to quantify and understand the changes in the viscoelastic parameters of the CTAT/NaCl/water samples due to the increased screening of intermicellar interactions as a result of the addition of salt.

4.1. Applicability of the Cox−Merz Rule. As discussed in section 3.2.2, viscoelastic gels usually follow the empirical Cox−Merz rule[9] (Figure 3b). The curves show an excellent superposition at $c_{NaCl} = 60$ mM ([NaCl]/[CTAT] = 1.42) over the entire range of ω and $\dot\gamma$. We notice significant deviations in the values of $\eta^*(\omega)/\eta_0$ and $\eta(\dot\gamma)/\eta_0$ at high ω and $\dot\gamma$ at very low and very high salt concentrations.

4.2. Existence of Three Regimes of Contrasting Flow Behaviors. Figure 4a shows the relaxation time τ_R, obtained using the relation $\tau_R \sim \omega_{co}{}^{-1}$, versus c_{NaCl}. On increasing c_{NaCl}, τ_R shows an initial increase, followed by a strong decrease. The dependence of τ_R on c_{NaCl} in these regimes may be fitted to the relation $\tau_R \sim c_{NaCl}{}^{\beta}$ (shown by solid lines in Figure 4a). The values of β is +0.11 for $c_{NaCl} \leq 2$ mM (regime I, [NaCl]/[CTAT] ≤ 0.05) and changes to −0.65 thereafter. The values of τ_R plotted in this figure are significantly larger than the values estimated from the fits to η^* versus ω that are exhibited in Table 1. This is because these fits estimate the average relaxation times, instead of the longest relaxation times. Fits to the low-frequency part of the G' and G'' versus ω data to the Maxwell model may be used to estimate the longest relaxation times.

Figure 4b shows the plots of the high-frequency plateau modulus G_0 obtained in the following ways: the values obtained from the Cole−Davidson fits (solid circles) and the values of $G'(\omega)$ at a high frequency $\omega = 29$ rads^{-1} (solid triangles). The two sets of values of G_0 deviate considerably at $c_{NaCl} \leq 2$ mM (regime I) but agree very well at higher salt concentrations ($c_{NaCl} \geq 5$ mM). At 5 mM ≤ c_{NaCl} ≤ 60 mM, G_0 increases with salt concentration, followed by a decrease at $c_{NaCl} \geq 60$ mM. These two regimes, characterized by different slopes (shown in Figure 4b and marked as regimes II and III), have been fitted to $G_0 \sim c_{NaCl}{}^{\beta'}$, where $\beta' = 0.31$ in regime II and −1.38 in regime III.

The same three regimes can be very clearly distinguished in Figure 4c, where η_0 is plotted versus c_{NaCl}. The values of η_0 are obtained from the fits of η^* (solid triangles) and $\eta(\dot\gamma)$ (solid circles) discussed above. η_0 shows an initial increase in regime I, followed by a weak decrease in regime II and subsequently a much stronger decrease in regime III. In all three regimes, η_0 has been fitted to the power law $\eta_0 \sim c_{NaCl}{}^{\beta''}$, where β'' is equal to 0.35 in regime I (fit

shown by dashed line), −0.29 in regime II (fit shown by solid line), and −2.04 in regime III (fit shown by dashed line). The weak increase in η_0 at low c_{NaCl} may be explained in terms of micellar growth as a result of enhanced screening of intermicellar interaction on the addition of NaCl. The subsequent decrease in η_0 at high c_{NaCl} may be explained in terms of intermicellar connections.[1,16,17] Fluorescence recovery after fringe pattern photobleaching (FRAPP) experiments have also shown an increase in the diffusion coefficients (i.e., a decrease in the effective viscosity) of aqueous, semidilute solutions of CTAT micelles in the presence of 0.1 and 1 M NaCl with increasing CTAT concentrations.[18] This effect increases with the increase in the salt concentration and has been explained in terms of connected micelles.

4.2.1. Connected Micelles. For suitably high concentrations of the added electrolyte, many of the measured rheological properties of entangled micellar solutions are found to deviate considerably from the predictions of the reptation−reaction theory.[2] Unusually high fluidity has been observed in aqueous micellar solutions of the system cetylpyridinium chlorate ($CPClO_3$)/sodium chlorate ($NaClO_3$).[19] For the system hexadecyltrimethylammonium bromide (CTAB)/potassium bromide (KBr)/water, Khatory et al. have observed anomalous scaling of the zero shear viscosity η_0 and the high-frequency plateau modulus G_0 with surfactant concentration.[16] The zero-shear viscosity η_0 of CTAC and NaSal shows a peak at [NaSal]/[CTAC] $\sim$ 0.6.[17] The increase and decrease of η_0 obey power-law scaling relations with CTAC concentration, characterized by exponents 1.1 and −2.1, respectively. A peak in the zero-shear viscosity has also been observed in aqueous solutions of CPyCl/NaSal at [NaSal]/[CPyCl] $\sim$ 1.[12] These results cannot be explained in terms of the theory for entangled micelles[5] but can be understood by considering intermicellar branching at high salt concentrations. These connections between micelles characterize a new relaxation process which involves the sliding of connections along the micelles.[20,21] The general features of stress relaxation seen in linear micelles are preserved in the case of branched micelles if one replaces the average length $\bar{L}$ by a new length $\bar{L}_c$, where $\bar{L}_c = [n_2/(n_1 + 2n_3)]l_p$.[16,21] In the expression for $\bar{L}_c$, l_p is the persistence length, n_1 is the concentration of the end-caps, n_2 is the number density of the persistence lengths, and n_3 is the number density of 3-fold network junctions. This model gives rise to a relaxation process that is faster than the predictions of the theory for reptation and reversible scission[5] and explains the anomalously high fluidity seen in some systems of wormlike micelles at high salt or surfactant concentrations.[16,17] These intermicellar connections serve as sliding contacts, aiding the faster reptation of the micelles and hence decreasing the viscosity of the system.[21] An interesting feature of our data is the existence of two distinct regimes (regimes II and III in Figure 4c) where η_0 shows a decrease with c_{NaCl}. In contrast to previous experiments with gemini surfactants,[3] there is a regime of weak decrease of η_0 (regime II) followed by a much stronger decrease on increasing c_{NaCl} (regime III). At the crossover between regimes II and III (c_{NaCl} = 60 mM), the change in the slope of η_0 (Figure 4c) is accompanied by a change in the sign of the slope of G_0, as shown in Figure 4b. In regime II, G_0 shows an anomalous increase with c_{NaCl}.

The increase in the plateau modulus G_0 with added salt concentration has been observed previously by earlier authors.[22−24] This effect has been explained in terms of the modification of the elastic properties of the micellar solution as a result of the intermicellar interactions between charged micelles, which leads to long-range strain fluctuations in the solution.

The addition of salt is known to encourage micellar growth.[2] However, as the CTAT concentration is fixed and lies in the semidilute regime, we do not expect ς, the correlation length of concentration fluctuations, to change appreciably. For flexible micelles, the correlation length ς is related to G_0 as $G_0 \sim ck_BT/l_e\xi^3$.[2,7] The entanglement length l_e scales with the persistence length l_p, and the correlation length ξ as $l_e \sim \xi^{5/3}/l_p^{2/3}$. An increase in G_0, therefore, implies a decrease in entanglement length l_e, which, in turn, implies an increase in the persistence length l_p. An increase in l_p is indicative of an increase in the surface charge of the micelles. Such an increase in the surface charge could occur due to the unbinding of the tosylate counterions from CTA^+ on the addition of NaCl.[25] Counterion unbinding could hence be another plausible explanation for the increase of G_0 with salt concentration. Low-frequency conductivity measurements have confirmed the phenomenon of counterion unbinding in the liquid crystalline phase of cesium perfluoro-octanol (CsPFO)/PFO/water on the addition of alcohol.[26] However, at $c_{NaCl} \geq$ 60 mM (regime III), the micelles are again screened completely, as indicated by the decrease in G_0 and η_0 in this regime. The decrease in viscosity of the system CTAC/NaSal with increasing concentrations of CTAC follows the relation $\eta_0 \sim c_{NaCl}{}^{\beta''}$, where $\beta'' = -2.1$,[17] very close to the value $\beta'' = -2.04$ obtained by us in regime III.

4.3. Superposition of the Linear and Nonlinear Rheology Data for CTAT/NaCl/Water. In this section, we discuss the superposition of the frequency response and flow curves of the CTAT/NaCl/water samples. In Figures 5 and 6, we have plotted master curves by normalizing the viscoelastic parameters by suitable quantities. The elastic and viscous moduli are normalized by η_0/τ_R, the dynamic viscosity η^* by $G_0\tau_R$, the shear stress σ by G_0, and both the shear rate $\dot{\gamma}$ and frequency ω by $\tau_R{}^{-1}$. Similar master curves for the linear rheology data of CTAT have been observed by Soltero et al.[27] on increasing the concentration of CTAT. In Figure 5, (a) and (b) correspond to the plots of the normalized $G''(\omega)$ and $G'(\omega)$ data, respectively, while Figure 5c shows the plots of the normalized dynamic viscosity $\eta^*(\omega)$. The curves for the normalized $G''(\omega)$ at 0 mM NaCl are found to deviate considerably from the master curve on which the data corresponding to $c_{NaCl} \geq$ 20 mM lie, which is indicative of a large difference in the viscous flow properties of CTAT in the screened and unscreened limits.

It is also possible to superpose the normalized stress σ/G_0 versus the normalized shear rate $\dot{\gamma}\tau_R$ plots of the CTAT/NaCl/water samples. All the flow curves are found to superpose very well in the regime of low $\dot{\gamma}\tau_R$ (Newtonian

(16) Khatory, A.; Lequeux, F.; Kern, F.; Candau, S. J. *Langmuir* **1993**, *9*, 1456.
(17) Aït Ali, A.; Makhloufi, R. *Phys. Rev. E* **1997**, *56*, 4474.
(18) Narayanan, J.; Manohar, C.; Langevin, D.; Urbach, W. *Langmuir* **1997**, *13*, 398.
(19) Appell, J.; Porte, G.; Khatory, A.; Kern, F.; Candau, S. J. *J. Phys. II France* **1992**, *2*, 1045.
(20) Drye, T. J.; Cates, M. E. *J. Chem. Phys.* **1992**, *96*, 1367.
(21) Lequeux, F. *Europhys. Lett.* **1992**, *19*, 675.
(22) Schmitt, V.; Lequeux, F. *J. Phys. II France* **1995**, *5*, 193.
(23) Candau, S. J.; Hebraud, P.; Scmitt, V.; Lequeux, F.; Kern, F.; Zana, R. *Nuovo Cimento* **1994**, *16D*, 1401.
(24) Oda, R.; Narayanan, J.; Hassan, P. A.; Manohar, C.; Salkar, R. A.; Kern, F.; Candau, S. J. *Langmuir* **1998**, *14*, 4364.
(25) Cates, M. E. Private communication.
(26) Li, Z.; Rosenblatt, C. *J. Chem. Phys.* **1998**, *89*, 5033.
(27) Soltero, J. F. A.; Puig, J. E.; Manero, O. *Langmuir* **1996**, *12*, 2654.

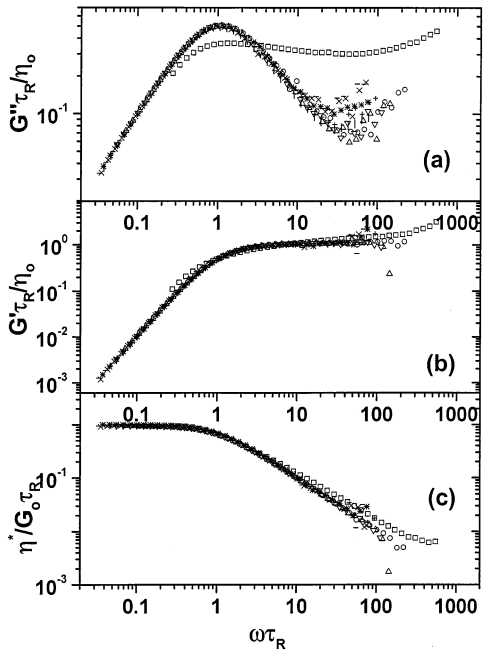

Figure 5. (a) and (b) show the values of $G''(\omega)$ and $G'(\omega)$, both scaled by η_0/τ_R, vs $\omega\tau_R$. Apart from the measurements with 0 mM NaCl (depicted by squares), all other curves lie on a master curve. (c) shows the scaled dynamic viscosity $\eta^*(\omega)/G_0\tau_R$ vs $\omega\tau_R$. In the diagrams, circles correspond to 20 mM NaCl, up-triangles to 40 mM, down-triangles to 60 mM, plus signs to 80 mM, cross signs to 90 mM, stars to 100 mM, and bars to 120 mM.

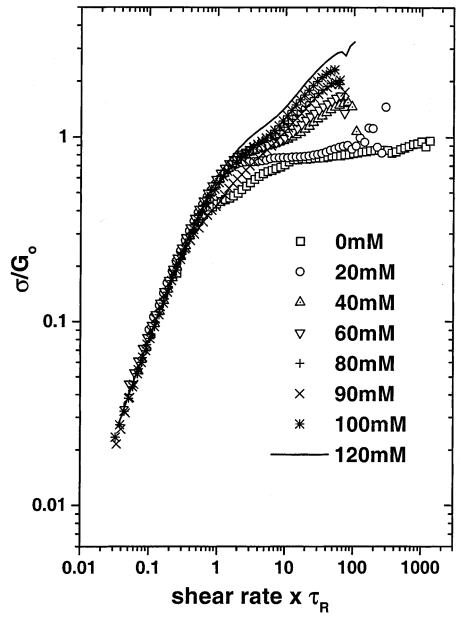

Figure 6. The normalized flow curves of CTAT (42 mM)/NaCl/water, where σ and $\dot{\gamma}$ are scaled as $\sigma \rightarrow \sigma/G_0$ and $\dot{\gamma} \rightarrow \dot{\gamma}\tau_R$. In the diagrams, squares stand for 0 mM NaCl while the keys for the other symbols are the same as in Figure 5. We have taken care to ensure that there is no expulsion of the sample from the cone and plate geometry during the flow curve measurements at high shear rates.

regime, characterized by unit slope of σ vs $\dot{\gamma}$ on a log−log plot) but show deviations at higher values of $\dot{\gamma}\tau_R$ (Figure 6). The normalized shear stresses do not overlap at $\dot{\gamma}\tau_R > 1$, with the slope of the flow curve increasing monotonically with increase in salt concentrations. This is extremely interesting in the light of previous experiments which find that shear banding in other micellar solutions such as CPyCl/NaSal is difficult to observe in systems with a broad distribution of relaxation times.[28−30] Our results encourage us to draw an analogy between the addition of salt and the increase in temperature in a wormlike micellar solution: the plateau in the nonlinear flow curve of CTAT + NaCl disappears at high salt content, very much like the observations of Porte et al., where they find that the plateau in the flow curve disappears on increasing the temperature.[31] Berret et al.[32] have observed perfect superposition for CPyCl/NaSal/water samples in the Newtonian regime of the flow curve, while the slope of the normalized stress in the plateau (nonlinear) regime increases on increasing the sample temperature. Interestingly, the branching of the micelles that we observe at $c_{NaCl} \geq 20$ mM does not have any significant effect on the master phase diagrams obtained from the linear rheology experiments (Figure 5). The normalized flow curves of CTAT/NaCl/water, however, show a significant change in the slope of the "plateau" region on increasing c_{NaCl}, which points to a change in the nonlinear flow behavior of the aqueous CTAT/NaCl samples on the addition of salt.

5. Conclusions

In this paper, we have discussed the modifications of the viscoelastic properties of CTAT (the concentration of CTAT is kept fixed at 42 mM) as a result of the addition of the salt. We find that the data may be divided into three distinct regimes, where η_0 and G_0 can be fitted to different power laws. The decrease of η_0 at high salt concentration has been explained in terms of intermicellar branching.[21] The anomalous increase of G_0 on increasing salt concentration has been explained in terms of tosylate unbinding from the CTA^+ on the addition of salt. It will be interesting to understand the precise mechanism of this counterion unbinding phenomenon. Significantly, at $c_{NaCl} = 60$ mM, the persistence length of the micelles is maximum, which indicates the presence of highly charged micelles at these concentrations. Interestingly, the scaling of τ_R on c_{NaCl} does not change from regime II to regime III. As shown in Figure 3, the superposition between $\eta^*(\omega)$ and $\eta(\dot{\gamma})$ is very good at $c_{NaCl} = 60$ mM.

The branching of the micelles does not appreciably alter the scaling of the linear rheology parameters (plots of normalized $G'(\omega)$, $G''(\omega)$, and $\eta^*(\omega)$ for $c_{NaCl} \geq 20$ mM, shown in Figure 5). In contrast, when the flow curves are superposed to lie on a single master curve, we find that the slope of the plateau increases on increasing c_{NaCl}, indicating a modification of the shear banding properties of the samples in the presence of intermicellar connections. Significant changes in the nonlinear flow behavior of cetyltrimethylammonium bromide (CTAB)/NaSal/water have been observed from small-angle light scattering experiments on increasing salicylate counterions.[33]

In light of the present work, it will be worthwhile to study more exhaustively the linear and nonlinear rheology of cylindrical micelles as a function of the surface charge, with and without multiconnected junctions. Anomalous

(28) Britton, M. M.; Mair, R. W.; Lambert, R. K.; Callaghan, P. T. *J. Rheol.* **1999**, *43*, 897.
(29) Callaghan, P. T.; Cates, M. E.; Rofe, C. J.; Smeulders, J. B. A. F. *J. Phys. II France* **1996**, *6*, 375.
(30) Bautista, F.; Soltero, J. F. A.; Perez-Lopez, J. H.; Puig, J. E.; Manero, O. *J. Non-Newtonian Fluid Mech.* **2000**, *94*, 57.
(31) Porte, G.; Berret, J. F.; Harden, J. L. *J. Phys. II France* **1997**, *7*, 459.
(32) Berret, J. F.; Porte, G.; Decruppe, J. P. *Phys. Rev. E* **1997**, *55*, 1668.
(33) Kadoma, I. A.; van Egmond, J. W. *Langmuir* **1997**, *13*, 4551.

flow properties of surfactant systems such as CPyCl/NaSal/water have been previously observed at about equimolar proportions of CPyCl and NaSal.[1,12] Till date, there have been several studies on the effect of the chemical formula and lipophilicity of the counterions on the growth of a micelle.[24,34] It will be extremely interesting to undertake a detailed study of the effects of the chemical nature of the counterion on its unbinding from a micelle.

Acknowledgment. The authors thank Professor M. E. Cates for useful discussions. They thank Professors S. Ramaswamy, P. R. Nott, and V. Kumaran for the use of the rheometer.

LA0203741

(34) Magid, L. J.; Hann, Z.; Warr, G. G.; Cassidy, M. A.; Butler, P. D.; Hamilton, W. A. *J. Phys. Chem. B* **1997**, *101*, 7919.